Seasonal and interannual variations of evaporation and their relations with precipitation, net radiation, and net carbon accumulation for the Gediz basin area

Bhaskar J. Choudhury
Hydrological Sciences Branch
Laboratory for Hydrospheric Processes
NASA Goddard Space Flight Center
Greenbelt, MD 20771, USA

Abstract

A model combining the rate of carbon assimilation with water and energy balance equations has been run using satellite and ancillary data for a period of 60 months (January 1986 to December 1990). Calculations for the Gediz basin area give mean annual evaporation as 395 mm, which is composed of 45% transpiration, 42% soil evaporation and 13% interception. The coefficient of interannual variation of evaporation is found to be 6%, while that for precipitation and net radiation are, respectively, 16% and 2%, illustrating that net radiation has an important effect in modulating interannual variation of evaporation. The mean annual water use efficiency (i.e., the ratio of net carbon accumulation and total evaporation) is ca. 1 g m^{-2} mm^{-1}, and has a coefficient of interannual variation of 5%. A comparison of the mean water use efficiency with field observations suggests that evaporation over the area is utilized well for biomass production. The reference crop evaporation for irrigated areas has annual mean and coefficient of variation as, respectively, 1176 mm and 3%. The total evaporation during three summer months of peak evaporation (June-August) is estimated to be about 575 mm for irrigated crops like maize and cotton. Seasonal variations of the fluxes are presented.

Keywords: Evaporation, Transpiration, Carbon assimilation, Net radiation, Satellite observations

1. Introduction

Total evaporation couples water and energy balance equations (Brutsaert, 1982), while transpiration, which is the major component of total evaporation over most of the land surface, is strongly linked with the rate of carbon assimilation (Tanner and Sinclair, 1983; Monteith, 1988). Consequently, it is desirable to consider carbon assimilation in doing energy and water balance calculations.

A biophysical process-based model, linking the rate of carbon assimilation with water and energy balance equations, described previously (Choudhury and DiGirolamo, 1998) has been run using spatially representative meteorologic and surface data for a period of 60 months (January 1986 to December 1990) over the global land surface. The essential aspects of the model and the data used in the calculations are presented below, while more details can be found in Choudhury and DiGirolamo (1998). Then, seasonal and interannual variations of evaporation and their relations with precipitation, net radiation, and net carbon accumulation over the Gediz basin area (38^{o}-39^{o}N, 27^{o}-28^{o}E) are presented and discussed.

2. Model, data, and uncertainties

2.1. Water balance equation

Daily change of root-zone available soil moisture has been calculated from the following equation:

$$W(j+1) = W(j) + P(j) + S_m(j) - I(j) - Q_S(j) - D(j) - E_S(j) - T(j) \quad (1)$$

where j is day number, W (j) is root zone available water at the beginning of day j, P (j) is precipitation, S_m (j) is snowmelt, I (j) is interception, Q_S (j) is surface runoff, D (j) is drainage out of the root-zone, E_S (j) is soil evaporation, and T (j) is transpiration for day j. All fluxes are expressed as daily totals in units of mm.

Note that precipitation is considered to provide all moisture at the surface (i.e., no irrigation or extraction of ground water for transpiration), and the sum of surface runoff and drainage constitutes total runoff.

An equation analogous to (1) is used to calculate daily change of water equivalent of snow, when present.

2.1.1. Components of total evaporation

Interception has been calculated using the Horton's model adopted for partial canopy cover:

$$I = f * \min (P, a P + b) \qquad (2)$$

where f is fractional vegetation cover, and a and b are parameters, which vary with vegetation type and rainfall intensity.

Soil evaporation is considered to occur in two stages: the energy limited rate or the exfiltration limited rate (Ritchie, 1972). The energy limited rate (E_{s1}) is calculated by adjusting evaporation (E_o) given by the Priestley and Taylor' (1972) equation for fractional exposed soil (1 - f):

$$E_{s1} = E_o (1 - f) \qquad (3)$$

The exfiltration limited rate (E_{s2}) is calculated from the Philip's equation (Ritchie, 1972):

$$E_{s2} = s [t^{0.5} - (t-1)^{0.5}] \qquad (4)$$

where s is the desorptivity and t is time (day number). The exfiltration limited rate is not allowed to exceed energy limited rate, and soil evaporation is assumed to be zero under snow-cover.

Transpiration under well-watered condition (T_u) is calculated from the Penman-Monteith equation (E_p), adjusted for fractional vegetation cover:

$$T_u = E_p f \qquad (5)$$

where E_p is given by,

$$E_p = \frac{\{ \Delta R_{ni} + \rho c_p D / r_e \}}{\lambda \{ \Delta + \gamma (r_c + r_H) / r_e \}} \qquad (6)$$

where λ is latent heat of vaporization, Δ is the slope of saturated vapor pressure with respect to air temperature, γ is psychrometer constant, R_{ni} is isothermal net radiation (i.e., surface temperature being equal to the air temperature), ρ is the density and c_p is the specific heat of air

at constant pressure, D is the vapor pressure deficit, r_e is the effective resistance for heat transfer, given by,

$$r_e^{-1} = r_H^{-1} + r_R^{-1} \quad (7)$$

where r_R is the longwave radiative transfer resistance, given by

$$r_R = \rho\, c_p / (4\, \sigma\, \varepsilon\, T_a^3) \quad (8)$$

σ is the Stefan-Boltzman constant, ε is the longwave emissivity and T_a is the air temperature, and r_H is the aerodynamic resistance for heat transfer, given by

$$r_H = ln (z / z_H) / (k\, u_*) \quad (9)$$

where z is the effective height where friction velocity (u_*) is determined, z_H is the roughness height for heat transfer and k is von Karman's constant, and r_c is the daytime mean canopy stomatal resistance for well-watered condition.

Considering the often observed linear correlation between leaf stomatal conductance (which is the inverse of stomatal resistance) and the rate of carbon assimilation (Yoshie, 1986; Marshall and Vos, 1991; Korner, 1994) and physiological link between canopy transpiration and carbon assimilation (Tanner and Sinclair, 1983; Monteith, 1988), r_c has been calculated from daytime mean rate of carbon assimilation by the canopy under well-watered condition (A_c) as:

$$r_c = y / A_c \quad (10)$$

where y is the slope relating leaf stomatal conductance to the assimilation rate. A_c has been calculated from the following equation (Spitters, 1986):

$$A_c = (A_m / \kappa)\, ln\, [(A_m + e_q\, a_l\, \kappa\, S) / \{ A_m + e_q\, a_l\, \kappa\, S\, (1\text{-}f) \}] \quad (11)$$

where A_m is the maximum leaf assimilation rate, κ is the extinction coefficient of photosynthetically active radiation (PAR) within the canopy, e_q is the quantum efficiency, a_l is PAR absorptance of a leaf and S is daytime mean PAR incident on the canopy.

The unstressed rates of transpiration and assimilation occur so long as the root-zone relative water content remains above 0.4, below which the rates are decreased linearly with the relative water content to provide the actual rates (Ritchie, 1981).

2.2. Energy balance equation

Net radiation (R_n), sensible (H) and soil heat (G) fluxes have been calculated following Budyko (1974) and Mintz and Walker (1993). The following equation is used to calculate G (W m^{-2}) for a month J:

$$G = 48.5 \, (T_a (J+1) - T_a (J-1)) / \Delta t \qquad (12)$$

where T_a (J+1) and T_a (J-1) are, respectively, the mean monthly air temperature of the months (J+1) and (J-1) and Δt is the number of days in the two months.

Then, R_n and H are obtained from the following equations:

$$R_n = \{ R_{ni} + (\lambda E + G) (r_H / r_R) \} / \{ 1 + (r_H / r_R) \} \qquad (13)$$

$$H = R_n - \lambda E - G \qquad (14)$$

where E is the total evaporation, and r_H and r_R are defined above (Eqs. 8 and 9).

2.3. Net carbon accumulation

The daily net carbon accumulation by plants (**C**) (also called the net primary productivity) is given by the difference of daily total gross assimilation ($\mathbf{A}_{g,t}$) and respiration (**R**) (Amthor, 1989):

$$\mathbf{C} = (\mathbf{A}_{g,t} - \mathbf{R}) \qquad (15)$$

where $\mathbf{A}_{g,t}$ is obtained by multiplying daytime mean rate of carbon assimilation by the canopy by the duration of daylight (Spitters, 1986), and **R** has been taken to be a constant fraction of $\mathbf{A}_{g,t}$ (Kira, 1975; Monteith, 1981; McCree, 1988).

2.4. Model parameters

All model parameters have been determined from published literature and these are given in Choudhury and DiGirolamo (1998). Spatial distribution of vegetation type dependent parameters has been prescribed using a land use and land cover data (Matthews, 1983).

2.5. Data for running the model

The data used to run the model are derived from satellite observations, four dimensional data assimilation procedure (4DDA) and ground measurements for a period of 60 months (January 1986 to December 1990). The mean monthly surface albedo, fractional cloud cover,

solar and photosynthetically active radiation were derived from the data produced under the International Satellite Cloud Climatology Project (Whitlock *et al.*, 1995; Choudhury and DiGirolamo, 1998). The mean monthly air temperature and vapor pressure have been derived from observations by the Tiros Operational Vertical Sounder (TOVS) on board NOAA satellites (Susskind *et al.*, 1997; Choudhury, 1997a). The friction velocity and surface air pressure are derived from a 4DDA (Schubert *et al.*, 1995). The monthly total precipitation values were produced under the Global Precipitation Climatology Project by merging gauge measurements and satellite observations, and were disaggregated into daily values (Meeson *et al.*, 1995; WCRP, 1996). The fractional vegetation cover has been derived from visible and near-infrared reflectances observed by the Advanced Very High Resolution Radiometer (AVHRR) on board NOAA satellites after correcting for sensor degradation and atmospheric effects (Choudhury and DiGirolamo, 1998).

These data have varied spatial resolution; highest resolution being 0.25^{o} x 0.25^{o} (latitude x longitude cell) for fractional vegetation cover and lowest being 2.5^{o} x 2.5^{o} for precipitation and vapor pressure deficit. Uncertainties in some of these data sets are can be found in Whitlock *et al.* (1995) and Choudhury (1997a). Calculations have been done at a daily time step and at 0.25^{o} x 0.25^{o} resolution; all data have been put in this time step and spatial resolution by duplicating their values within their own resolution.

2.6. Model initialization

The water balance calculation requires an initial value of available moisture { Eq. 1; W (j=1) } at all spatial grids. Since there are no measurements of this moisture over the global land surface, it was set at half the maximum value to run for the five years. The moisture values obtained at the end of this five-year run were then used to calculate the fluxes presented below (i.e., the results from the second five-year run). While this procedure minimizes the arbitrariness of the initial choice of the moisture value, uncertainties in the fluxes still remain for the first few months.

2.7. Uncertainties in the results

Comparisons with micrometeorologic measurements at two locations, estimates of evaporation by the atmospheric water budget method for six river basins (areas ca. 1-7 x 10^6 km^2) and water balance of 132 catchments (areas ca. 1-10^3 km^2) having different vegetation cover distributed throughout the world and 10 river basins (areas ca. 1-7 x 10^6 km^2) gave uncertainties of about 15% and 20%, respectively, for annual and monthly evaporation (Choudhury and DiGirolamo, 1998; Choudhury, 1999). The partitioning of total evaporation into transpiration, soil evaporation and interception was also consistent with available data. The magnitude of error in net radiation has not yet been determined lacking meaningful comparisons with spatially representative observed values (such measurements are now being done, which will allow error analysis).

Choudhury and DiGirolamo (1998) found good agreement between the computed and observed (neutron probe) average soil moisture in the top 1 m at 12 fairly well distributed grass-covered locations within Illinois (38^{o}-42^{o}N, 88^{o}-90^{o}W) for a period of 24 months (1987-1988). This comparison for the present 60 months period is shown in Fig. 1. Fig. 1a shows the mean seasonal variation (arithmatic average of five yearly values for each month) of the measured soil moisture and the computed available moisture (note different scales in the figure). The data presented by Hollinger and Isard (1994) suggest the wilting point moisture to be about 190 mm. If this wilting point moisture (190 mm) is subtracted from the measured values, the computed values agree well with the estimated available moisture during the spring, but they are lower by 40-60 mm during summer and fall. This difference between the seasonal variation of the computed and estimated available moisture could be related to vegetation-type dependent moisture extraction pattern; a significant part of the area over which these measurements have been made is planted to maize, which extracts more moisture during the summer than grass (see Fig. 4 in, Doorenbos and Pruitt, 1977). A linear regression analysis of these 60 months of moisture values gave an explained variance of 73% and a slope of 1.25 (scatter plot not shown). To assess the extent by which the model is providing interannual variations, the soil moisture

anomalies were computed by subtracting the mean seasonal variation from the monthly values. The computed and observed moisture anomalies are in good agreement; the explained variance being 50% and slope being 0.78 (Fig. 1b).

Since none of the error estimates reported above is based upon comparisons done by calibration (or adjustment) of the model parameters, these estimates suggest the likely uncertainties in the model results for areas where it has not been tested, but satisfy the basic assumptions (viz., no irrigation or extraction of ground water for transpiration) to a reasonable degree.

3. Results and discussion

Because of interannual variations of the weather, it is pertinent to put the weather conditions of the present 60 months in the context of climatology. Thus, Fig. 2 shows the mean and the range of air temperature and monthly total precipitation over the Gediz basin area (38^{o}-39^{o}N, 27^{o}-28^{o}E) together with the climatologic data at Izmir (38.5^{o}N, 27.3^{o}E) from Muller (1982); the climatology for air temperature and precipitation are, respectively, for 39 and 58 years. It is desirable to put solar radiation also in this perspective, but I could not find such measurements. It is seen in Fig. 2 that, with respect to the climatology, the present air temperature values are generally lower by about 0.5^{o}C, and the mean precipitation values are also lower (maximum difference being 30 mm for January), except for July and August (the months of minimum precipitation) and November. While the mean values of precipitation for the present 60 months do not generally match the climatologic mean values, it is comforting to see that the climatologic mean values are always within the range of present data.

Fig. 3 shows the mean and the range of monthly total evaporation and water equivalent of net radiation. The maximum net radiation is seen to occur during May-July period (about one to two months before the maximum air temperature or minimum precipitation, Fig. 2), while peak evaporation occurs in May. A comparison of the seasonal pattern of evaporation with that of net radiation and precipitation (Fig. 2) shows that evaporation is being determined by both the available energy and moisture. While precipitation decreases in going from January to May,

evaporation increases with increasing available energy by depleting soil moisture. However, evaporation does not increase with increasing precipitation during fall and winter due to a lack of energy. The evaporative fraction (which is the ratio of evaporation and net radiation) is close to one during winter (November-January), but decreases to about 0.5 during May and further to about 0.1 during August-September.

Seasonal variations of the mean and range of fractional transpiration and soil evaporation are shown in Fig. 4. The fractional transpiration decreases, while fractional soil evaporation increases in going from July to August, due to soil water stress affecting transpiration. The fractional transpiration begins to increase from October, reaching its mean maximum value (0.61) in May, when fractional soil evaporation reaches its mean minimum value (0.34). It is also seen that mean fractional transpiration exceeds fractional soil evaporation only for four months (April-July), which will appear to be an important period for the vegetation community relying on precipitation in this area. This is more clearly seen from the seasonal variation of net carbon accumulation by the plant communities, where the peak month is seen to be May and then the rate decreases rapidly due to decreasing soil moisture (Fig. 5).

The annual values of the fluxes and fractional transpiration and soil evaporation are summarized in Table 1. The coefficient of interannual variation is highest for precipitation (16%), followed by fractional soil evaporation (8%), total evaporation (6%), fractional transpiration (5%), net carbon accumulation (4%) and net radiation (2%). It is perhaps understandable that the interannual variation of soil evaporation follows that of precipitation because of intermittent wetting and drying processes determining soil evaporation. Also, the interannual variation of fractional transpiration and net carbon accumulation might be expected to be similar because fractional vegetation cover is an important determinant of both. Considering that the coefficient of variation of evaporation is 6%, while that for precipitation and net radiation are, respectively 16% and 2%, it appears that net radiation has an important effect in modulating the variability of evaporation. The mean annual water use efficiency (which is the ratio of net carbon accumulation and total evaporation) is found to ca. 1 g (carbon) m^{-2}

mm^{-1}, and has a coefficient of interannual variation of 5%. The mean efficiency corresponds to about 2.2 g (dry matter) m^{-2} mm^{-1} if carbon content of vegetation is taken to be 45% of dry matter (Ajtay *et al.*, 1979). Although this mean efficiency is within the range of observations {ca. 1-5 g (dry matter) m^{-2} mm^{-1} }, it is at the high end of values for many plant communities (Choudhury, 1997b). This suggests that evaporation over the Gediz basin area is utilized well for biomass production.

The results presented above would have to be modified for irrigated areas. The model calculations could be repeated knowing the time and the amount of water applied. Methodologies for determining these irrigation characteristics from satellite observations have not yet been developed. Alternately, evaporation from well-watered crops could be estimated knowing crop coefficient and reference crop evaporation from planting to harvest (Doorenbos and Pruitt, 1977; Allen et al., 1996). While the crop coefficients cannot yet be determined from satellite observations, areally representative values of reference crop evaporation can be obtained from these observations (Choudhury, 1997a). Seasonal variation of the mean and the range of the reference crop (grass) evaporation values for the Gediz basin area is shown in Fig. 6. The mean maximum evaporation (184 mm mo^{-1}) occurs in July, while mean minimum (37 mm mo^{-1}) occurs in December. The mean total evaporation during the peak three months (June-August) is 500 mm, with the range 482-510 mm. For crops like maize and cotton, evaporation during these three months could be about 575 mm, if the mid season crop coefficient is taken to be 1.15 (Allen et al., 1996). The mean and coefficient of variation of annual reference crop evaporation are, respectively, 1176 mm and 3%.

4. Summary and conclusions

A biophysical process-based model, linking the rate of carbon assimilation with water and energy balance equations, was run using satellite, assimilated and surface observations for 60 months (January 1986 to December 1990) to obtain components of total evaporation, net radiation and net carbon accumulation.

Calculations show that seasonal variation of total evaporation over the Gediz basin area is determined by available energy and moisture. The evaporative fraction (which is the ratio of total evaporation and net radiation) is close to 1.0 during the winter (November-January), but decreases to about 0.5 during May and further to about 0.1 during August-September. The mean maximum total evaporation and net carbon accumulation occur during May. Transpiration is the dominant component of total evaporation during four months (March-June).

The mean annual evaporation over the area is found to 395 mm, which is composed to 45% transpiration, 42% soil evaporation and 13% interception. The coefficient of interannual variation is highest for precipitation (16%) and lowest for net radiation (2%), while it is 6% for total evaporation. The mean annual water use efficiency (which is the ratio of net carbon accumulation and total evaporation) is found to be 1 g (carbon) m^{-2} mm^{-1}. Considering that this value of the efficiency is at the high end of the values for many plant communities, it appears that evaporation over this area is utilized well for biomass production.

Seasonal variation of the mean and the range of the reference crop (grass) evaporation is given, which could be adjusted by crop coefficients for estimating evaporation from irrigated areas.

Acknowledgement

Data processing assistance was provided by Nick DiGirolamo.

References

Allen, R. G., Smith, M., Pereira, L. S., Pruitt, W. O., 1996. Proposed revision to the FAO procedure for estimating crop water requirements. Proc. 2nd Int. Symp. Irri. Hort. Crops, Crete.

Ajtay, G. L., Ketner, P., Duigneand, P., 1979. Terrestrial primary production and phytomass. In: Bolin, B., Degans, E. T., Kempe, S., Ketner, P. (Eds.). The Global Carbon Cycle, John Wiley, New York, pp. 129-181.

Amthor, J. S., 1989. Respiration and Crop Productivity. Springer-Verlag, New York.

Brutsaert, W., 1982. Evaporation into the Atmosphere. Reidel Publication, Boston.

Budyko, M., 1974. Climate and Life. Academic Press, New York.

Choudhury, B. J., 1997a. Global pattern of potential evaporation calculated from the Penman-Monteith equation using satellite and assimilated data, Remote Sens. Environ., 61, 64-81.

Choudhury, B. J., 1997b. Estimating areal evaporation using multispectral satellite observations. In: Sorooshian, S., Gupta, H. V., Rodda, J. C. (Eds.). Land Surface Processes in Hydrology, Springer-Verlag, New York, pp. 347-382.

Choudhury, B. J., 1999. Evaluation of an empirical equation for annual evaporation using field observations and results from a biophysical model, J. Hydrol., (in press).

Choudhury, B. J., DiGirolamo, N. E., 1998. A biophysical process-based estimate of global land surface evaporation using satellite and ancillary data. I. Model description and comparison with observations, J. Hydrolo., 205, 164-185.

Doorenbos, J., Pruitt, W. O., 1977. Crop water requirements. FAO Irrigation and Drainage Paper 24, Food and Agriculture Organization of the United Nations, Rome, 144 pp.

Hollinger, S. E., Isard, S. A., 1994. A soil moisture climatology of Illinois, J. Clim., 7, 822-833.

Kira, T., 1975. Primary production of forests. In: Cooper, J. P. (Ed.). Photosynthesis and Productivity in Different Environments, Cambridge University Press, New York, pp. 5-40.

Korner, Ch., 1994. Leaf diffusive conductances in the major vegetation types of the globe. In: Schulze, E. -D., Caldwell, M. M. (Eds.). Ecophysiology of Photosynthesis, Springer-Verlag, New York, pp. 463-490.

Marshall, B., Vos, J., 1991. The relation between the nitrogen concentration and photosynthetic capacity of potato (*Solanum tuberosum* L.) leaves, Ann. Bot., 68, 33-39.

Matthews, E., 1983. Global vegetation and land use: New high-resolution data bases for climate studies, J. Clim. Appl. Meteorol., 22, 474-487.

McCree, K. J., 1988. Sensitivity of sorghum grain yield to ontogenic changes in respiration coefficients, Crop Sci., 28, 114-120.

Meeson, B. W., Corprew, F. E., McManus, J. M. P., Myers, D. M., Closs, J. W., Sun, K. -J., Sunday, D. J., Sellers, P. J., 1995. ISLSCP Initiative I- global data sets for land-atmosphere models, 1987-1988, Goddard Space Flight Center, MD.

Mintz, Y., Walker, G. K., 1993. Global fields of soil moisture and land surface evapotranspiration derived from observed precipitation and surface air temperature, J. Appl. Meteorol., 32, 1305-1334.

Monteith, J. L., 1981. Climatic variation and growth of crops, Q. J. R. Meteorol. Soc., 107, 749-774.

Monteith, J. L., 1988. Does transpiration limit the growth of vegetation or vice versa?, J. Hydrol., 100, 57-68.

Muller, M. J., 1982. Selected climatic data for a global set of standard stations for vegetation science. Dr. W. Junk, The Hague.

Priestley, C. H. B., Taylor, R. J., 1972. On the assessment of surface heat flux and evaporation using large-scale parameters, Mon. Wea. Rev., 100, 81-92.

Ritchie, J. T., 1972. Model for predicting evaporation from row crop with incomplete cover, Water Resour. Res., 8, 1204-1213.

Ritchie, J. T., 1981. Water dynamics in the soil-plant-atmosphere system, Plant Soil, 58, 81-96.

Schubert, S., Park, C. -K., Wu, C. -Y., Higgins, W., Kondratyeva, Y., Molod, A., Takacs, L., Seablom, M., Rood, R., 1995. A multiyear assimilation with the GEOS-1 system: overview and results, NASA TM-104606, Goddard Space Flight Center, Greenbelt, Maryland, pp. 183.

Spitters, C. J. T., 1986. Separating the diffuse and direct component of global radiation and its implication for modeling canopy photosynthesis. II. Calculation of canopy photosynthesis, Agric. For. Meteorol., 38, 231-242.

Susskind, J., Piraino, P., Rokke, L., Iredell, L., Mehta, A., 1997. Characteristics of the TOVS Pathfinder Path A data set, Bull. Am. Meteorol. Soc., 78, 1449-1472.

Tanner, C. B., Sinclair, T. R., 1983. Efficient water use in crop production: research or re-search, In: Taylor, H. M., Jordan, W. R., Sinclair, T. R. (Eds.). Limitations to Efficient Water Use in Crop Production, American Society of Agronomy, Madison, pp. 1-28.

WCRP, 1996. GEWEX data sets, GEWEX News, 6, 7-10.

Whitlock, C. H., Charlock, T. P., Staylor, W. F., Pinker, R. T., Laszlo, I., Ohmura, A., Gilgen, H., Konzelman, T., DiPasquale, R. C., Moats, C. D., LeCroy, S. R., Ritchey, N. A., 1995. First global WCRP shortwave surface radiation budget dataset, Bull. Am. Meteorol. Soc., 76, 905-922.

Yoshie, F., 1986. Intercelluar CO_2 concentration and water-use efficiency of temperate plants with different life-forms and from different microhabits, Oecologia, 68, 370-374.

Table 1. A summary of annual values of the fluxes and some fractions. The summary given are mean, range and coefficient of variation (c.v., %) for precipitation (P, mm), water equivalent of net radiation (R_n, mm), total evaporation (E, mm), net carbon accumulation (NCA, t (carbon) ha^{-1}), fractional transpiration (f_T) and soil evaporation (f_{Es}).

	P	R_n	E	NCA	f_T	f_{Es}
Mean	533	959	395	3.94	0.45	0.42
Range	437-613	925-977	364-417	3.71-4.11	0.42-0.48	0.38-0.46
c.v.	15.8	2.1	5.6	4.3	5.4	8.0

Caption to the figures

Figure 1. Computed and observed soil moisture within Illinois during January 1986 to December 1990, (a) mean seasonal variation, and (b) moisture anomalies. Note different scales for seasonal variation of observed soil moisture and computed *available* moisture. The wilting point moisture needs to be subtracted from the observed values for them to be comparable to the computed values. The results of least square linear regression for moisture anomalies are given in the figure.

Figure 2. Seasonal variation of the mean and range of daily mean air temperature and monthly total precipitation for the present 60 months of data for the Gediz basin area (38^{o}-39^{o}N, 27^{o}-28^{o}E). Also shown are the climatologic mean values at Izmir (38.5^{o}N, 27.3^{o}E).

Figure 3. Seasonal variation of the mean and range of monthly total evaporation and water equivalent of net radiation for the present 60 months of data.

Figure 4. Seasonal variation of the mean and range of fractional transpiration and soil evaporation.

Figure 5. Seasonal variation of the mean and range of net carbon accumulation.

Figure 6. Seasonal variation of the mean and range of reference crop (grass) evaporation for the Gediz basin area.

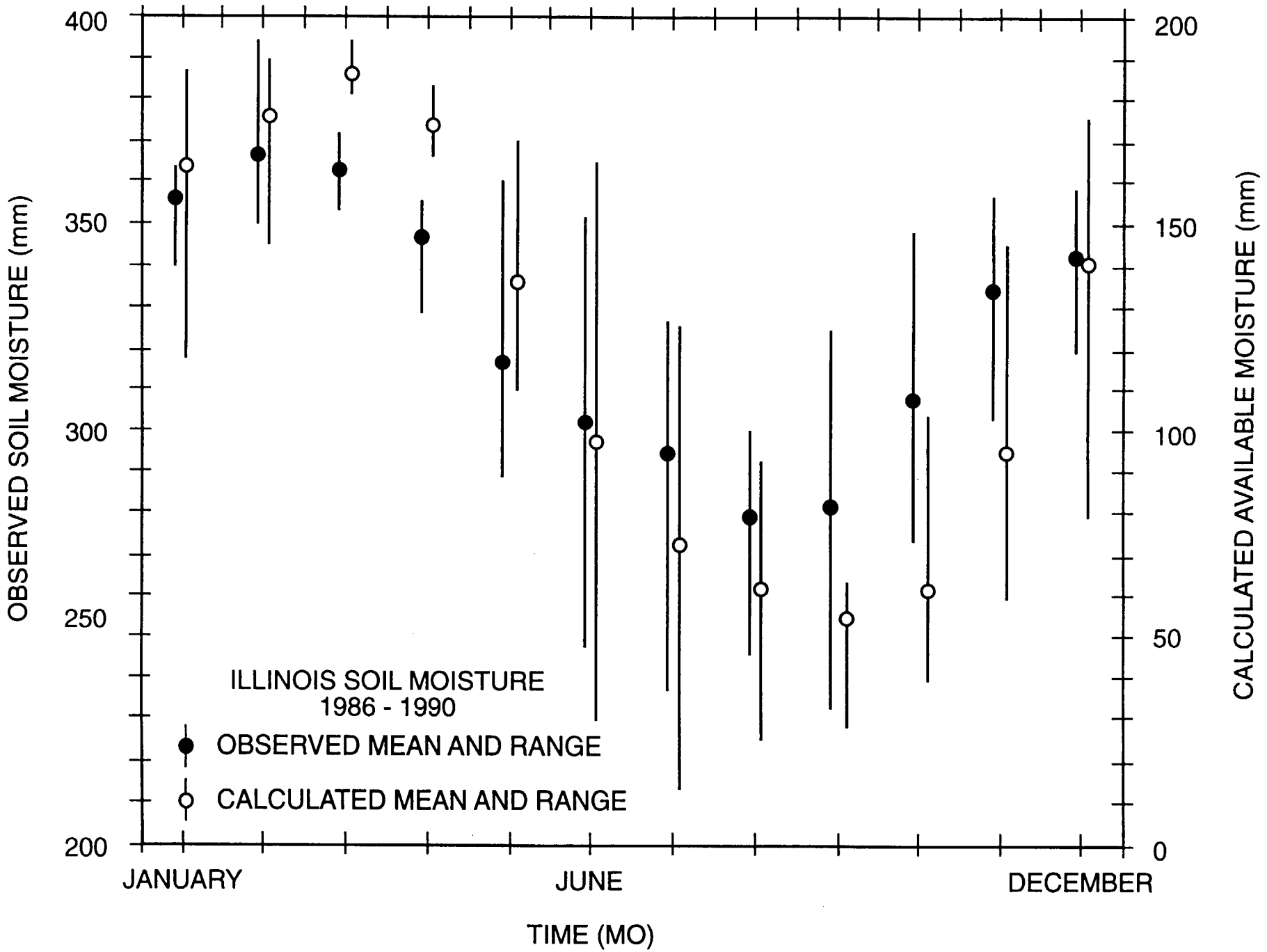

Fig. 18

L1129.001

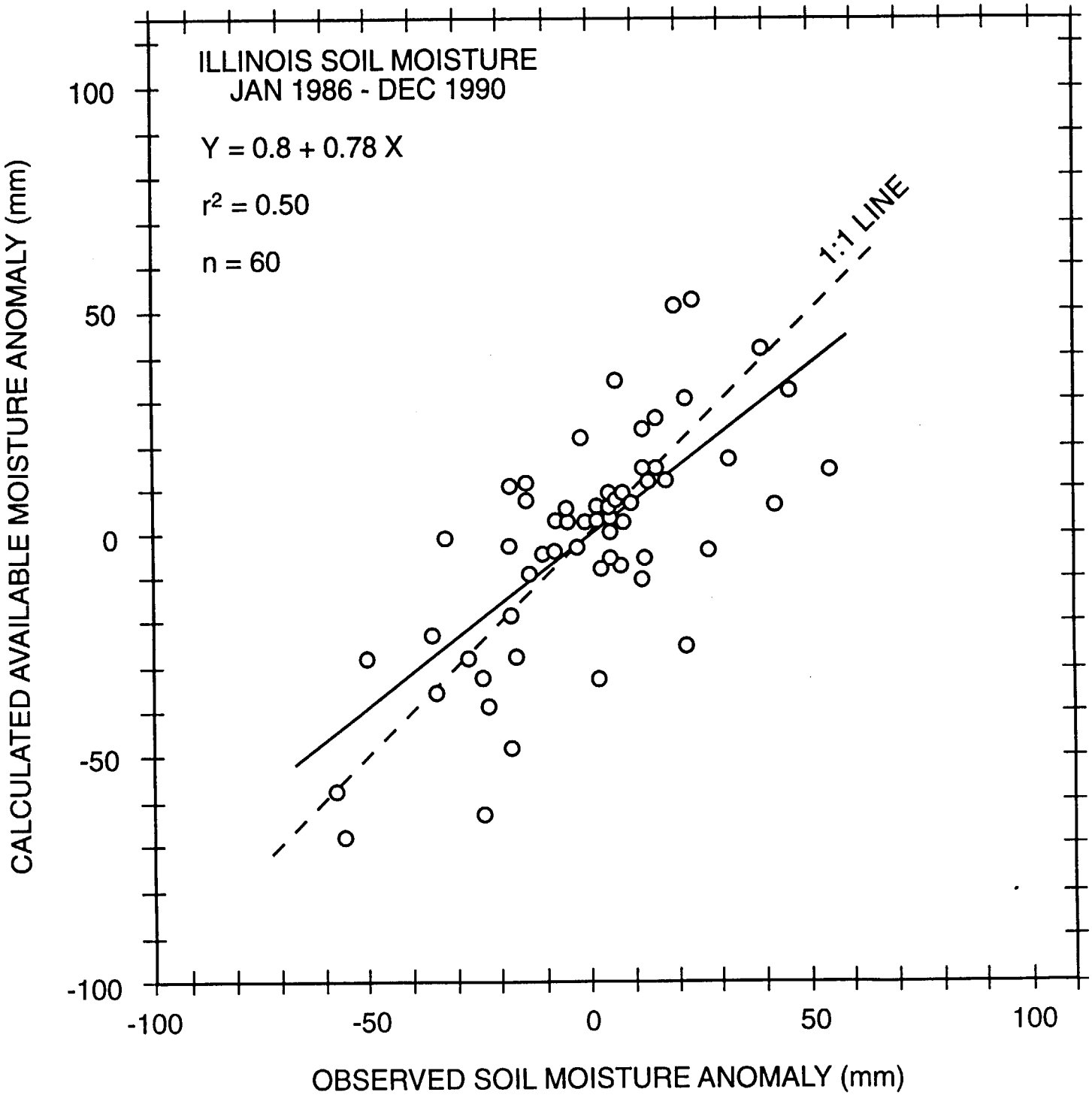

Fig 16

L1129 003

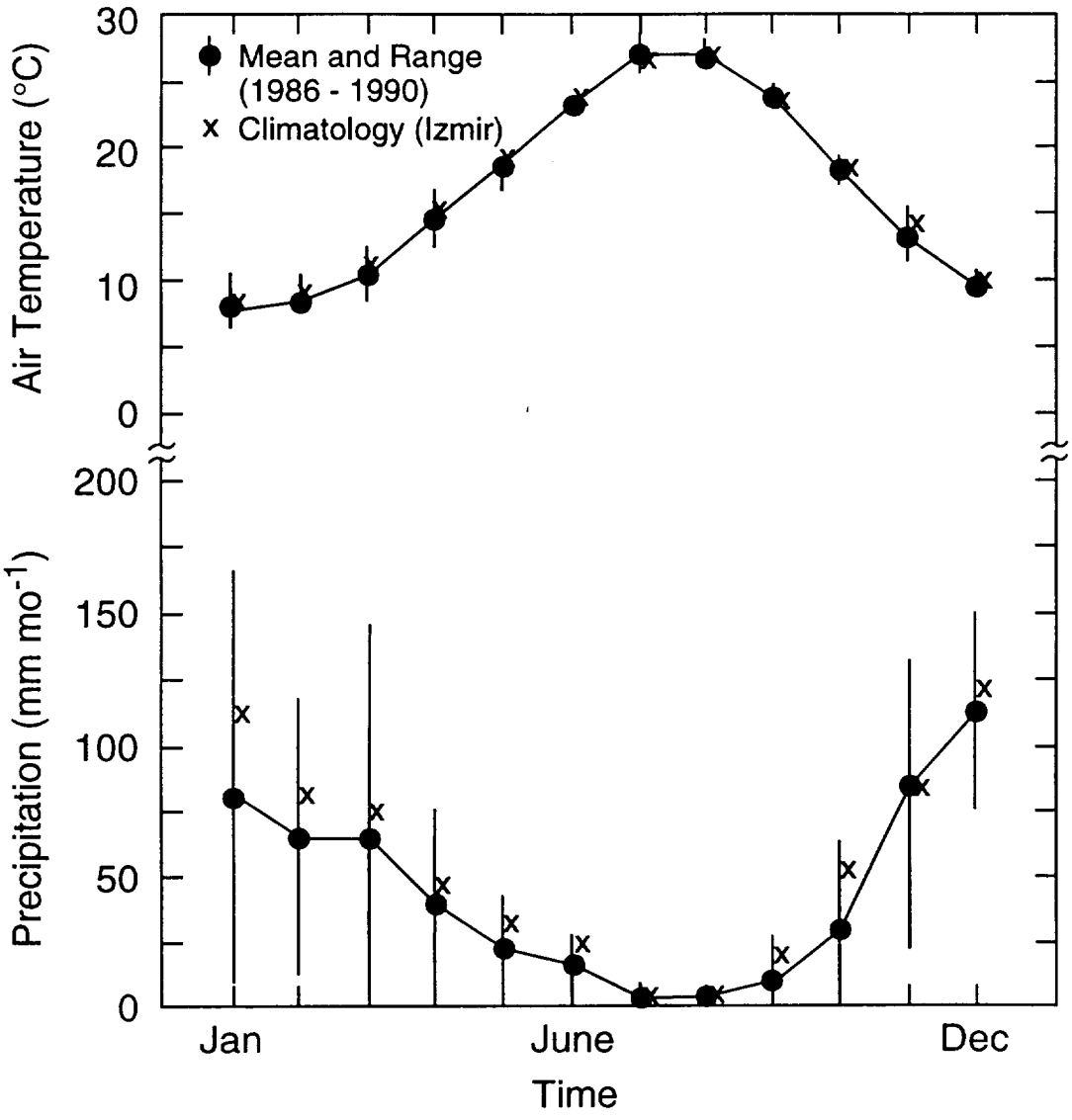
Air Temperature (°C)
30
20
10
0
Mean and Range
(1986 - 1990)
x Climatology (Izmir)
Precipitation (mm mo-1)
200
150
100
50
0
Jan
June
Dec
Time

Fig. 2

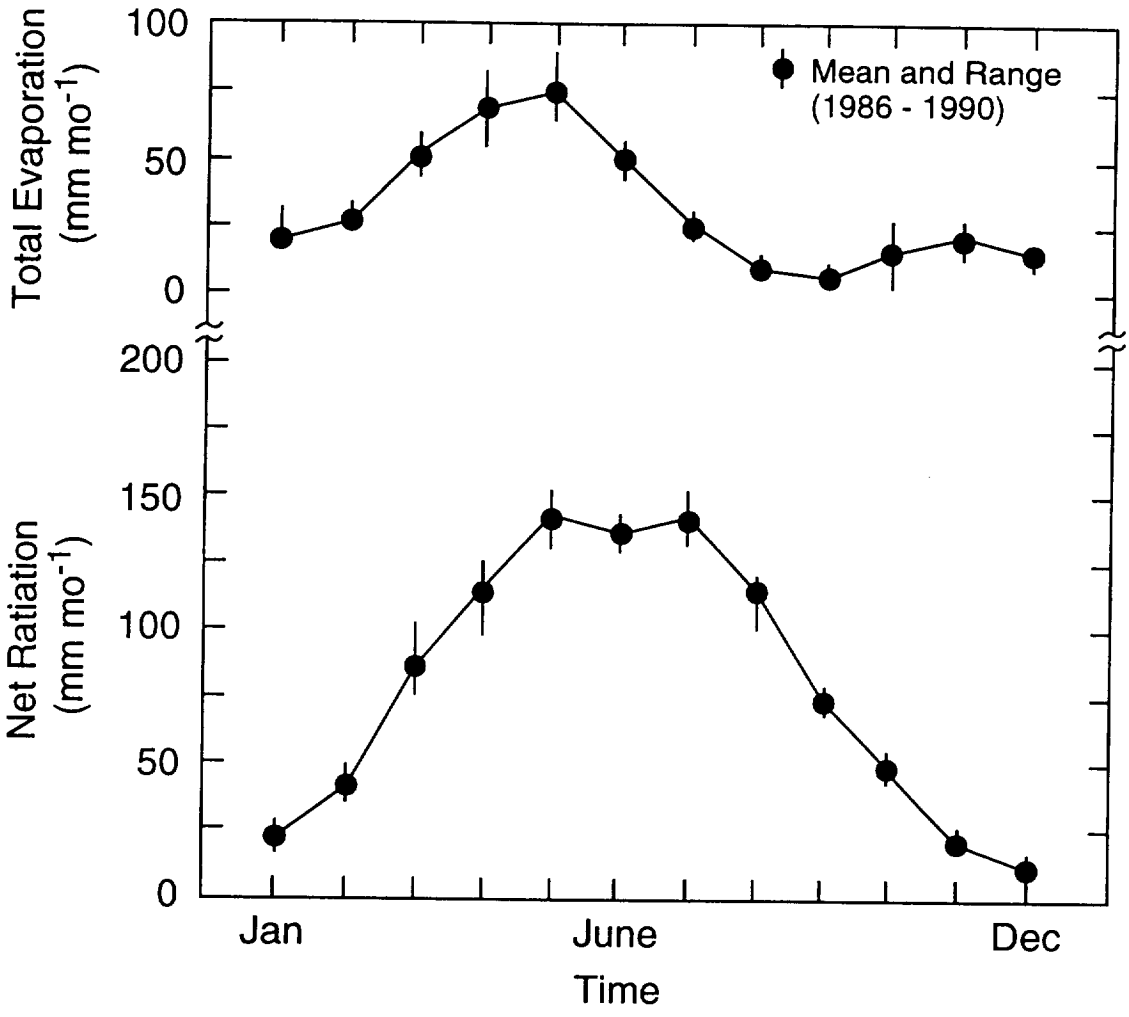

P1129.003

Fig. 3

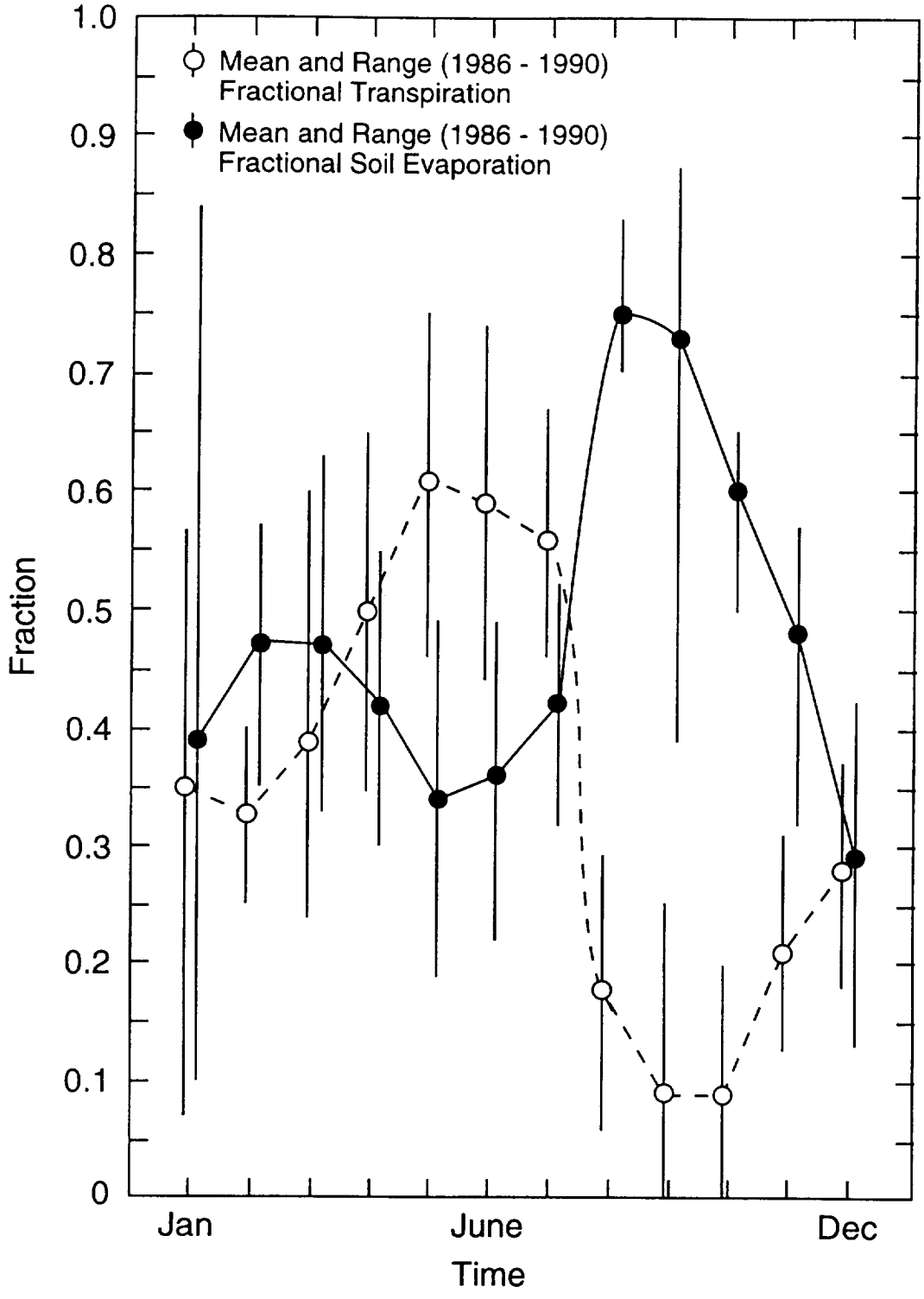

P1129.002

Fig. 4

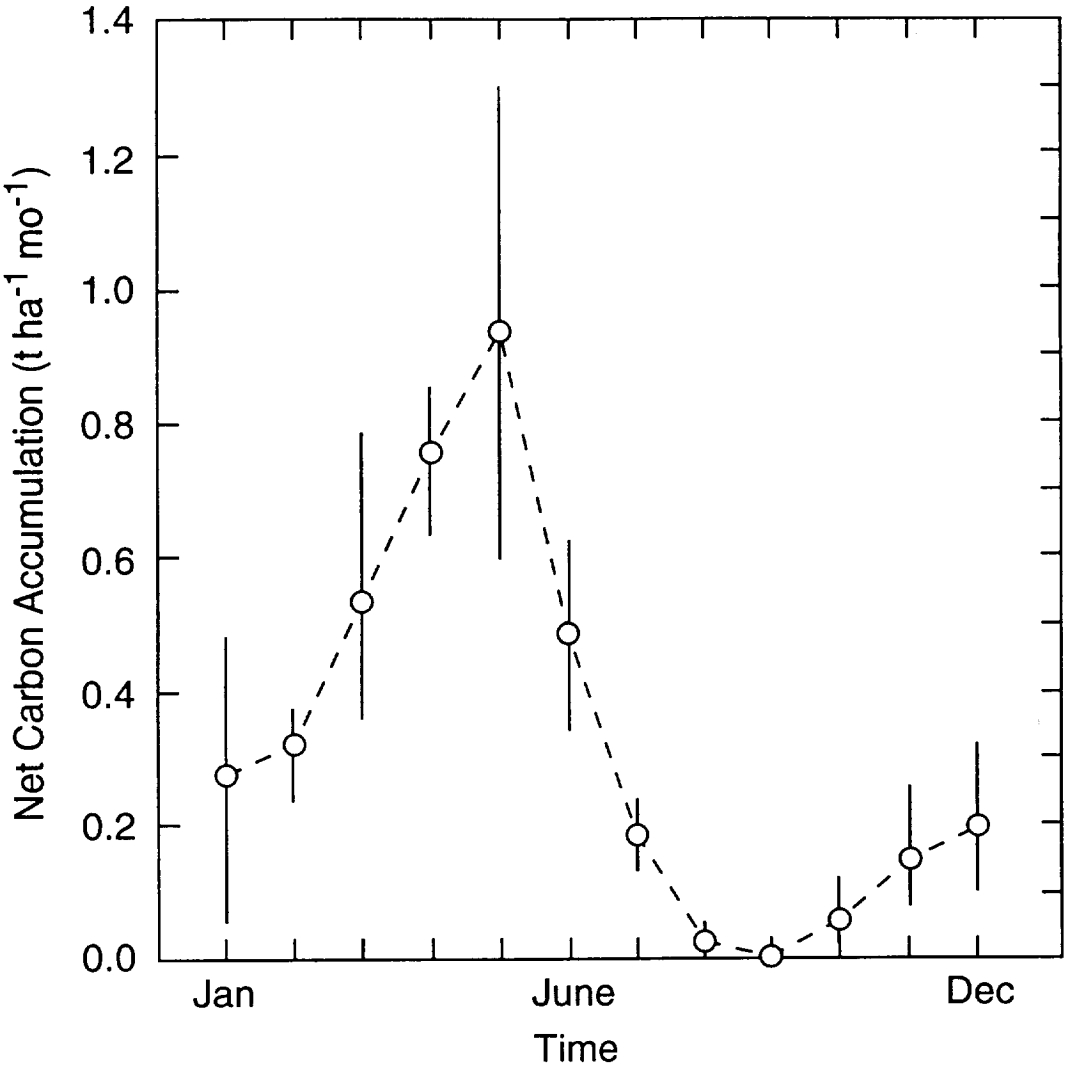
1.4
1.2
1.0
0.8
0.6
0.4
0.2
0.0
Net Carbon Accumulation (t ha-1 mo-1)
Jan
June
Dec
Time

Fig. 5

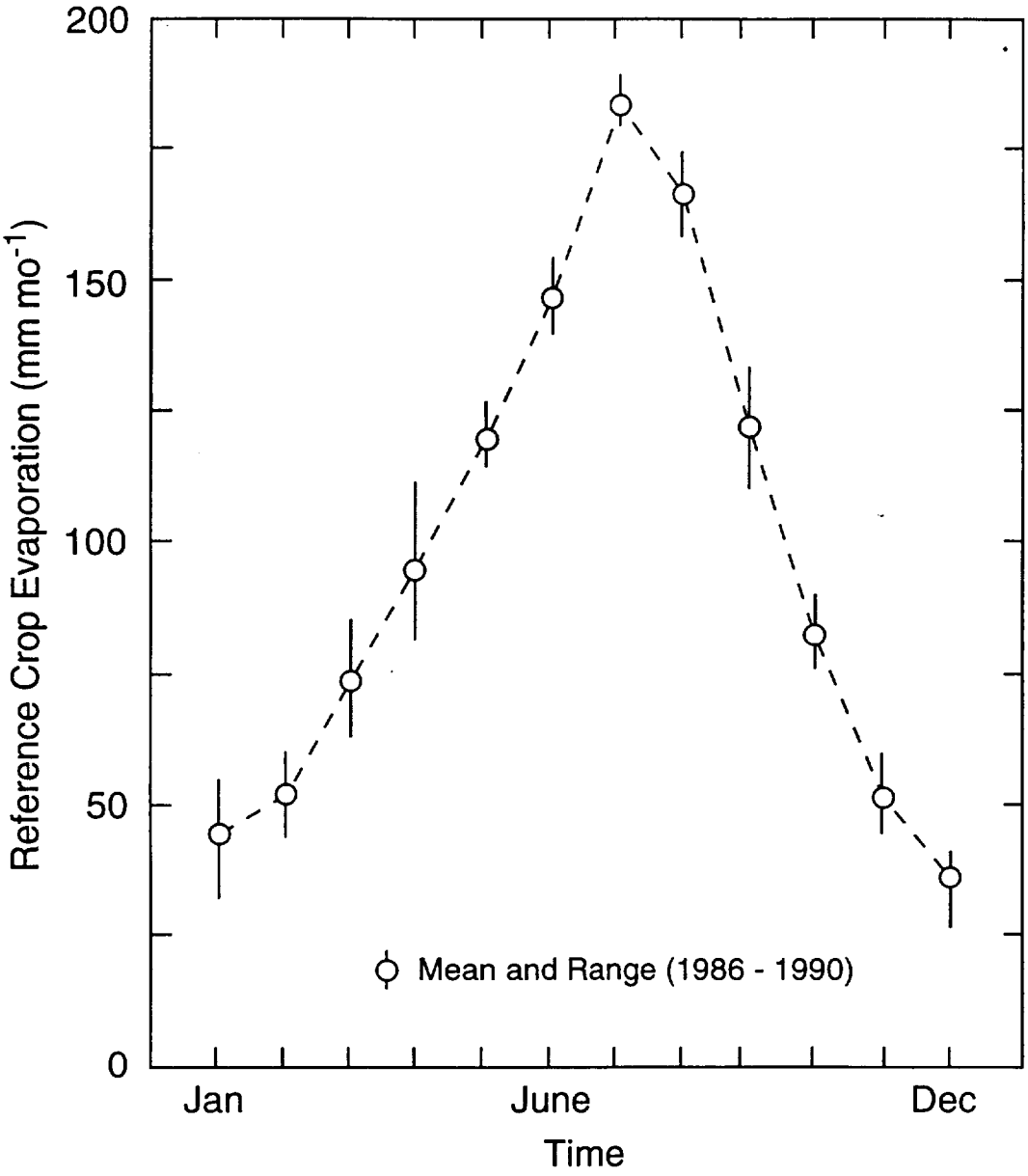

Q1129.001

Fig. 6